

INVESTIGATION ON THE MICROWAVE PULSE SIGNAL COMPRESSION WITH NGD CIRCUIT

B. Ravelo

IRSEEM (Research Institute on Electronic and Embedded Systems)
EA 4353, at Graduate School of Engineering ESIGELEC
Technopole du Madrillet, Av. Galilée, BP 10024
76801 Saint Etienne du Rouvray Cedex, France

Abstract—This paper demonstrates the exhibition of pulse compression from an electronic circuit with negative group delay (NGD). This circuit consists of a field effect transistor (FET) cascaded with shunt RLC network. Theoretic and experimental investigations have proved that, at its resonance frequency, the group delay of this circuit is always negative. The present study shows that around this resonance, it presents a gain form enabling to generate pulse compression. To validate this concept, as proof-of-principle, devices with one- and two-stages FET were implemented and tested. Measurements of the one-stage test device evidenced an NGD of about -2.5 ns and simultaneously with 2 dB amplification operating at 622 MHz resonance frequency. In the frequency domain, in the case of a Gaussian input pulse with 40 MHz frequency standard deviation, this resulted in 125% expansion of pulse width compared to the input one. In time domain, simulations showed that the compression was about 80% in the case of an input Gaussian pulse with 4 ns standard deviation. With the other prototype comprised of two-stage NGD cell, the use of a sine carrier of about 1.03 GHz allowed to achieve 87% pulse width compression.

1. INTRODUCTION

Three decades since the 1980s, various techniques of pulse compression (PC) have been developed at optical- and microwave-wavelengths and with both low- and high-wave power devices in order to convert a long-duration pulse of microwave power into a shorter one. It should be

noted that the principles and methods that have been proposed depend on the field of applications [1–3]. PC was applied, at first, to ultra-fast laser systems [4–6], and then its use has become more and more common thanks to the development of chirped pulse amplification [7–11]. Then, PC effect was realized in a Mach-Zehnder-interferometer geometry by passing a broadband ultra-short pulse through two chirped fiber Bragg gratings with different chirp rates [12]. Owing to the great interest for the development of radar and communication systems, the PC has been used to improve the range resolution. In other respects, a microwave pulse compressor based on a passive resonant cavity has been investigated by several authors [13–15], in order to increase microwave power. The prerequisites are that the compressor cavity must present a high Q-factor, the constituting waveguides should operate with an oversized mode of the field in order to increase the power strength, and the power microwave sources should be narrow-band. This combination of requirements is ensured in quasi-optical cavities and particularly in ring-shaped multi-mirror cavities, where the energy is sent into the cavity via corrugated mirror [16–18]. But in practice, the implementation of such a technique remains generally very complicated and at high cost.

Much simpler PC technique based on negative group delay (NGD) structure was recently proposed [19]. Theoretic investigations towards the design of passive- [20–24] and active- [25–31] circuits have been made during the last two decades, and the NGD phenomenon has been evidenced by many relevant experiments. In the 1990s [25–27], Chiao's group introduced an NGD topology of active circuit similar to the resonant atomic system with a negative refractive index and based on the use of an operational amplifier in negative feedback with a passive system composed of R , L and C [28–31]. But, generally, such a topology is frequency-limited and difficultly integrable [25–31]. In the same period, Lucyszyn and co-workers [20] proposed an NGD synthesizer operating at microwave frequencies. Otherwise, in the early 2000s, Eleftheriades and co-workers introduced a microwave passive circuit exhibiting NGD at some GHz [22–24]. This circuit was originally deduced from the analogy of the metamaterial composed of an array of thin metallic wires combined with split ring resonators [32]. As demonstrated by Pendry and Smith at the end of the 1990s, these artificial materials can simultaneously exhibit negative permittivity and negative permeability at their resonance frequencies [32–36]. Nevertheless, these NGD passive structures are not suitable for microwave applications because of the narrow bandwidth and excessive losses systematically associated to the generation of significant NGD. Till 2005, the existing NGD devices were limited in either operating

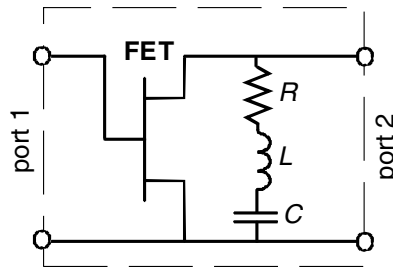


Figure 1. NGD active cell for the microwave signals.

frequency band, or attenuation.

To overcome such problems, a simple topology of NGD active cell depicted in Figure 1 has been proposed and developed [37–40]. This structure is composed by a field effect transistor (FET) in cascade with shunt RLC series network.

The synthesis relations allowing the calculation of the R , L , and C elements of this NGD cell were established in [38]. The present study demonstrates, at first, by theory and through experiments that, as expected, such an NGD cell can be used to achieve a PC function; the approach is similar to that one developed in [19]. Compared to the other available techniques [1–19], the presented one is endowed with numerous assets: ease of design, size reduction, implementation at low cost, and ability to compensate for losses and to operate at low and high frequencies.

The theoretic analysis presented in this paper describes why and how this NGD active circuit described in Figure 1 behaves as a microwave compressor. To illustrate this PC effect, a modulated Gaussian pulse centered at the resonance frequency of the NGD circuit is considered. Then, this compression effect is confirmed by a very good agreement found between, at first, the theoretic approach and the results of simulations made with ADS microwave circuit simulator from AgilentTM prior to validation through measurements. Thanks to this PC function, this active circuit could be potentially utilized for the microwave signal integrity improvement. As example, mostly because of electromagnetic dispersion effects, pulse expansions can be induced by the channel dispersion and also the electromagnetic interference (EMI) in certain telecommunication systems. Furthermore, in these areas, the NGD function permits also a priori, to reduce for propagation delay.

For the sake of completeness, pieces of information about the analytical approach of the NGD cell under study and already available

in the literature will have to be repeated. Section 2 introduces the expansion of insertion gain $|S_{21}|$, around $\omega_0 = 1/\sqrt{LC}$ by use of Taylor's series expansion in order to establish the condition required to realize PC with this active cell. To validate the proposed PC concept, simulation and experimental works were performed and discussed in Section 3. Finally, the conclusion of this paper is drawn in the last section.

2. THEORETICAL EVIDENCE OF THE PC EFFECT

In the same way as in [19], in order to prove the principle of this compression phenomenon, let us consider the input signal assumed as a modulated Gaussian wave pulse with a carrier angular frequency equal to $\omega_0 = 1/\sqrt{LC}$ expressed as:

$$x(t) = e^{-\frac{(t-t_0)^2}{2\Delta T_x^2} + j\omega_0 t}, \quad (1)$$

where ΔT_x is the standard deviation (half width at $1/e$ of the maximal input value), t_0 is the central time of the Gaussian and $j = \sqrt{-1}$. It ensues that the Fourier transform of such a signal is defined as:

$$X(j\omega) \approx \sqrt{2\pi} \cdot \Delta T_x \cdot e^{-\frac{1}{2}\Delta T_x^2(\omega-\omega_0)^2 - j(\omega-\omega_0)t_0}. \quad (2)$$

According to the signal processing theory, this function is also Gaussian, and its angular frequency standard deviation is:

$$\Delta\omega_x = \frac{1}{\Delta T_x}. \quad (3)$$

It means that the PC in time domain involves a pulse expansion in frequency domain and vice versa. This is why in this study, the standard deviation of the Gaussian output is compared, at first, theoretically, with the input one through the transmittance of the circuit under investigation written as:

$$H(j\omega) = S_{21}(j\omega) = \frac{-2Z_0 \cdot g_m \cdot R_{ds} \left[R + j\left(L\omega - \frac{1}{C\omega}\right) \right]}{Z_0 \cdot R_{ds} + (Z_0 + R_{ds}) \left[R + j\left(L\omega - \frac{1}{C\omega}\right) \right]}. \quad (4)$$

To highlight this analytical approach, let us consider the black box system shown in Figure 2.

As its transfer function $H(j\omega)$ is excited by $X(j\omega)$, the output Fourier transform is:

$$Y(j\omega) = H(j\omega) \cdot X(j\omega) = e^{\ln|H(j\omega)| + j\text{Arg}[H(j\omega)]} \cdot X(j\omega). \quad (5)$$

A simplified and approximated analytical study is proposed hereafter in order to interpret the behaviour of this output in a more logic way.

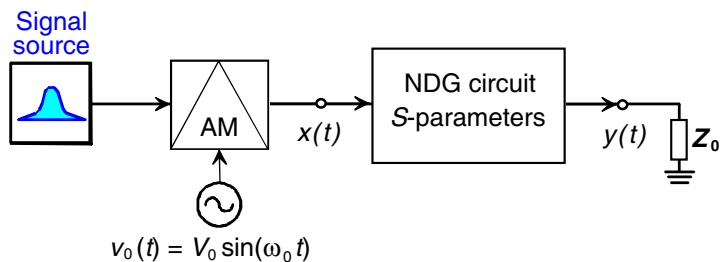


Figure 2. Block diagram of the understudy configuration in time-domain with $Z_0 = 50 \Omega$.

The Taylor’s series expansion is considered, first, of the magnitude $\ln |H(j\omega)|$ denoted $\ln |H_a(j\omega)|$, around the resonant angular frequency, ω_0 :

$$\ln |H_a(j\omega)| \approx \ln |H(\omega_0)| + \frac{H'(\omega_0)}{H(\omega_0)}(\omega - \omega_0) + \frac{1}{2} \frac{H''(\omega_0)}{H(\omega_0)}(\omega - \omega_0)^2 + O[(\omega - \omega_0)^3], \tag{6}$$

where $H'(\omega_0)$ and $H''(\omega_0)$ are respectively the first- and second-order derivatives of $|H(j\omega)|$ with respect to ω . Then, the application of the same procedure to the transmission phase defined as $\varphi(\omega) = \angle S_{21}(j\omega)$ leads to the following approximated expression of the approximated expression denoted $\varphi_a(\omega)$ given by:

$$\begin{aligned} \varphi_a(\omega) &\approx \varphi(\omega_0) + \varphi'(\omega_0)(\omega - \omega_0) + \frac{1}{2} \varphi''(\omega_0)(\omega - \omega_0)^2 + O[(\omega - \omega_0)^3] \\ &= \varphi(\omega_0) - \tau(\omega_0)(\omega - \omega_0) - \frac{1}{2} \tau'(\omega_0)(\omega - \omega_0)^2 + O[(\omega - \omega_0)^3]. \end{aligned} \tag{7}$$

Knowing that at resonance, $\varphi(\omega_0) = 0$ and in the vicinity of resonance ω_0 , $\tau'(\omega_0) \approx 0$ is obtained, this implies that:

$$\varphi_a(\omega) \approx -\tau(\omega_0)(\omega - \omega_0) + O[(\omega - \omega_0)^3]. \tag{8}$$

It should be noted that higher order terms can be ignored if the input signal bandwidth is small enough. As this phase response is relatively linear, the $Y(j\omega)$ -magnitude is unaffected. So, the output modulus can be defined as:

$$|Y(j\omega)| \approx |H(\omega_0)| e^{\frac{H'(\omega_0)}{H(\omega_0)}(\omega - \omega_0) + \frac{H''(\omega_0)}{2H(\omega_0)}(\omega - \omega_0)^2} \cdot |X(j\omega)|. \tag{9}$$

By substituting for $X(j\omega)$ from Equations (2) into (9), the above expression can be rewritten as:

$$|Y(j\omega)| \approx \sqrt{2\pi} |H(\omega_0)| \cdot \Delta T_x \cdot e^{\frac{H'(\omega_0)}{H(\omega_0)}(\omega - \omega_0) - \frac{1}{2} \left[\Delta T_x^2 - \frac{H''(\omega_0)}{H(\omega_0)} \right] (\omega - \omega_0)^2}. \tag{10}$$

It is worth recalling that through determination the insertion gain magnitude $|H(j\omega)|$ resulting from Equation (4), it can be established that:

$$|H(\omega_0)| = \frac{2g_m R_{ds} Z_0 R}{R_{ds} R + Z_0 (R + R_{ds})}, \quad (11)$$

$$H'(\omega_0) = \left. \frac{\partial |H(j\omega)|}{\partial \omega} \right|_{\omega=\omega_0} = 0, \quad (12)$$

$$\begin{aligned} |H(\omega_0)|'' &= \left. \frac{\partial^2 |H(j\omega)|}{\partial \omega^2} \right|_{\omega=\omega_0} \\ &= \frac{8g_m R_{ds}^2 Z_0^2 L^2 [R_{ds} Z_0 + 2R(Z_0 + R_{ds})]}{R [R_{ds} R + Z_0 (R + R_{ds})]^3} > 0. \end{aligned} \quad (13)$$

And thus, the output amplitude in Equation (10) can be simplified as follows:

$$|Y(j\omega)| \approx |H(\omega_0)| \Delta T_x \sqrt{2\pi} e^{-\frac{1}{2} \left[\Delta T_x^2 - \frac{H''(\omega_0)}{H(\omega_0)} \right] (\omega - \omega_0)^2}. \quad (14)$$

It should also be noticed that according to the value or more precisely the sign of the quantity $\Delta T_x^2 - \frac{H''(\omega_0)}{H(\omega_0)}$, three different types of frequency responses, $Y(j\omega)$ are distinguished.

2.1. Case 1: $\Delta T_x^2 - \frac{H''(\omega_0)}{H(\omega_0)} < 0 \quad \Leftrightarrow \quad \Delta T_x < \sqrt{\frac{H''(\omega_0)}{H(\omega_0)}}$

In this case, the input bandwidth $\Delta\omega_x$ becomes generally too large. It can be observed that the approximated output expressed in Equation (14) is physically meaningless because the hypothesis of second order limited expansion introduced in Equations (6) and (8) is no longer valid. So, analysis from the exact or more accurate consideration of $H(j\omega)$ is rather necessary. In fact, it can be found that the $|Y(j\omega)|$ -behaviour is widely different to the Gaussian spectrum. Hence, there is no conservation of the signal integrity. Therefore, the comparison between the $x(t)$ -input, and $y(t)$ -output pulse widths remains analytically very complicated.

2.2. Case 2: $\Delta T_x^2 - \frac{H''(\omega_0)}{H(\omega_0)} = 0 \quad \Leftrightarrow \quad \Delta T_x = \sqrt{\frac{H''(\omega_0)}{H(\omega_0)}}$

In this case, mathematically, the singular case of constant spectrum $|Y(j\omega)| \approx \sqrt{2\pi} |H(\omega_0)| \cdot \Delta T_x$ appears and by inverse Fourier transform, it implies that in time domain, output signal $y(t)$ is given by:

$$y(t) \approx |H(\omega_0)| \Delta T_x \delta[t - t_0 - \tau(\omega_0)]. \quad (15)$$

But, this result is not veritably realistic because first, the input spectrum given by $|X(j\omega)|$ and then, the output one $|Y(j\omega)|$ are practically limited in terms of frequency bandwidth.

2.3. Case 3: $\Delta T_x^2 - \frac{H''(\omega_0)}{H(\omega_0)} > 0 \Leftrightarrow \Delta T_x > \sqrt{\frac{H''(\omega_0)}{H(\omega_0)}}$

The present case constitutes the only adequate requirement permitting to achieve correctly the PC under a practical situation with validity of the second order expansion suggested formerly because the output Fourier transform expressed in Equation (14) behaves as a Gaussian pulse:

$$|Y(j\omega)| \approx Y_{\max} e^{-\frac{(\omega-\omega_0)^2}{2\Delta\omega_y^2}}, \tag{16}$$

having an amplitude:

$$Y_{\max} = \frac{2\sqrt{2\pi}g_m \cdot R_{ds} \cdot Z_0 \cdot R \cdot \Delta T_x}{R_{ds} \cdot R + Z_0(R + R_{ds})}, \tag{17}$$

and an angular frequency standard deviation:

$$\Delta\omega_y = \frac{1}{\sqrt{\Delta T_x^2 - \frac{H''(\omega_0)}{H(\omega_0)}}} = \frac{\Delta\omega_x}{\sqrt{1 - \frac{H''(\omega_0)}{H(\omega_0) \cdot \Delta T_x^2}}}, \tag{18}$$

obviously, under the following condition:

$$\Delta T_x > \Delta T_{x \min} = \sqrt{\frac{H''(\omega_0)}{H(\omega_0)}} \Leftrightarrow \Delta\omega_x < \frac{1}{\Delta T_{x \min}}. \tag{19}$$

Theoretically, by using in Equation (19) the expressions given in expressions (11) and (13), the minimal input standard deviation allowing the generation of compression phenomenon with the cell shown in Figure 1 should be:

$$\Delta T_{x \min} = \frac{2L\sqrt{R_{ds} \cdot Z_0 [R_{ds} \cdot Z_0 + 2R(Z_0 + R_{ds})]}}{R [R_{ds} \cdot R + Z_0(R + R_{ds})]}. \tag{20}$$

Furthermore, it can be observed that under condition (19), the pulse width is expanded in frequency domain ($\Delta\omega_y > \Delta\omega_x$). To sum up, the approximated output inferred by inverse Fourier transform of Equation (16) is written as:

$$y(t) = \frac{|H(\omega_0)|\Delta T_x}{\sqrt{\Delta T_x^2 - \frac{H''(\omega_0)}{H(\omega_0)}}} e^{-\frac{[t-t_0-\tau(\omega_0)]^2}{2\left[\Delta T_x^2 - \frac{H''(\omega_0)}{H(\omega_0)}\right]}} \cdot e^{j\omega_0 t}, \tag{21}$$

it can be seen that this output behaves as a modulated Gaussian whose standard deviation is:

$$\Delta T_y = \sqrt{\Delta T_x^2 - \frac{4L^2 R_{ds} Z_0 [R_{ds} Z_0 + 2R(Z_0 + R_{ds})]}{R^2 [R_{ds} R + Z_0 (R + R_{ds})]^2}}. \quad (22)$$

So, under the condition set in Equation (19), the objective of the study expressed as $\Delta T_y < \Delta T_x$. Hence, practically, it means that the pulse width is compressed in time-domain. Furthermore, compared to input signal $x(t)$, output signal $y(t)$ is amplified by the quantity:

$$\alpha = \frac{\Delta T_x}{\Delta T_y} |H(\omega_0)|. \quad (23)$$

However, as reported in [19], it is worth underlining that when ΔT_x approaches to $\Delta T_{x \min}$, a significant PC occurs. At this stage, prior to the discussion of our experimental results, let us describe the design process of the NGD devices presented in this paper.

3. VALIDATIONS OF THE PROPOSED PC CONCEPT

First and foremost, the simulations and designs of the tested circuits presented in this section were performed with microwave and electronic simulator ADS from AgilentTM.

3.1. Design Process

The flow chart shown in Figure 3 summarizes the sequence of actions developed to design the NGD active circuits. It should be noted that the process proposed in this paper is well-suited to the use of classical electronic circuit commercial simulators/designers. Moreover, we should keep in mind that the design of complex circuits such as those found in most of the microwave active devices requires the use of speed computers, and the tools available for computation can sometimes affect the responses obtained from simulations. The technique used to design these devices is similar to the well-known cases of modern classical microwave devices as filter, amplifier, coupler. . . .

At first, the electrical requirements have to be tight to meet the pre-set frequency response, in particular the fixed NGD level. Then, an ideal-circuit model can be drawn by using the synthesis relations introduced in [37, 38]. To be more realistic, it is worth taking into account a reliable (complete linear or non-linear) model of the employed FET including bias network, the effects of layout interconnect lines and the actual manufacturing details. So, the use of an electromagnetic simulation tool such as Momentum from

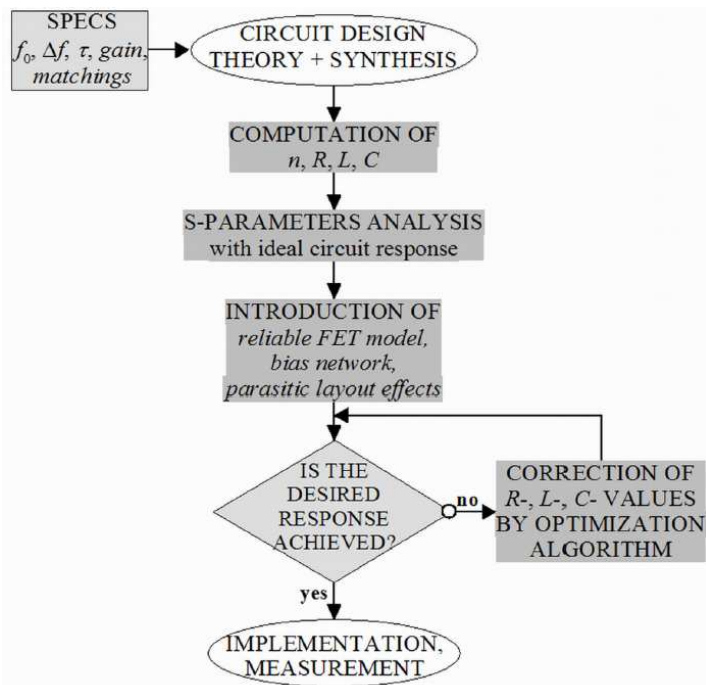


Figure 3. Design flow of the NGD device (n is the number of NGD cells).

ADS is necessary to reach good performances. To get acceptable final responses, numerical optimizations may be needed prior to implementation and measurements.

To verify the aforementioned theoretical predictions about pulse signal compression as proof-of-principle, two different devices were designed, fabricated and studied; they consisted of a NGD circuit with an FET and three resonant cells in cascade and a two-stage NGD active device investigated in [37–39].

3.2. Experimental Results with One Stage NGD Device: Demonstration of Pulse Signal Compression through Time Domain Analysis

Figure 4 shows the layout of the designed hybrid planar circuit printed on FR4 substrate with relative permittivity $\epsilon_r = 4.3$ and height $h = 800 \mu\text{m}$. It mainly consists of an FET ATF-34143 from Avago TechnologyTM in inductive bias with power consumption $V_d = 2 \text{ V}$ and

$I_d = 100$ mA cascaded with three shunt RLC series resonant cells. This configuration was chosen in order to validate the PC effect and as well as the NGD effects, with the components available.

The transconductance $g_m = 226$ mS and the drain-source resistance $R_{ds} = 27 \Omega$ were extracted through the FET ATF-34143 S -parameters of the non linear model provided by the manufacturer. Therefore, one gets the S -parameter measurement results viewed in Figure 5.

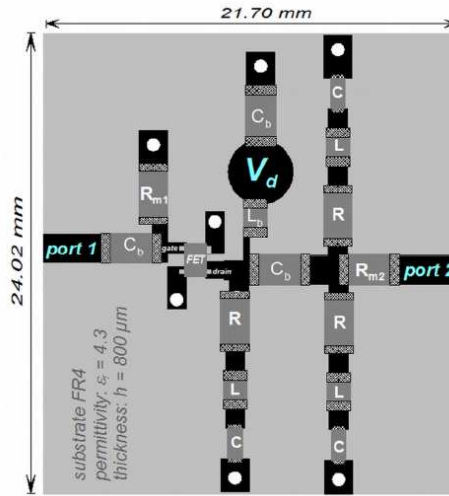


Figure 4. Layout of the fabricated active device using an FET ATF34143, $R_{m1} = 82 \Omega$, $R_{m2} = 22 \Omega$, $R = 18 \Omega$, $L = 51$ nH, $C = 0.5$ pF, $C_b = 1$ nF, $L_b = 220$ nH.

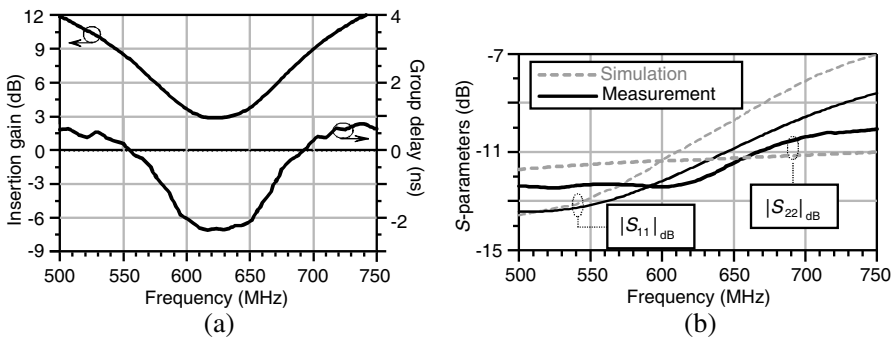


Figure 5. Measured results: (a) Insertion gain S_{21} dB/group delay, and (b) S -parameters S_{11} dB and S_{22} dB.

Figure 5(a) shows that, in a frequency band of about 135 MHz width centered at around 622 MHz, the gain and group delay are better than 2 dB and -2 ns, respectively. In the same frequency band, Figure 5(b) indicates that the matching level for this NGD device is better than -9 dB.

In order to better understand the significance of these frequency results, time-domain measurements were made with a modulated Gaussian wave pulse (8.4 ns as standard deviation) having at 622 MHz carrier. Figure 6 shows that the output behaves as a Gaussian pulse, slightly compressed because of the gain shape around the resonance.

The presented transient simulation was run using the measured S -parameters and a Gaussian input pulse with standard deviation was $\Delta T_x = 4$ ns and modulated by a sine carrier frequency, $f_0 = 622$ MHz according to the configuration shown in Figure 2. In frequency domain, it gives a Gaussian pulse with $\Delta f_x = 40$ MHz as frequency standard deviation. Consequently, as shown in Figure 7, the resulting output spectrum can be approximated to a Gaussian pulse with a frequency standard deviation of about $\Delta f_y = 50$ MHz (or $\Delta T_x = 3.3$ ns).

The output pulse width is thus expanded about 125% and amplified about 3.86 dB with respect to the input pulse one. As plotted in Figures 8(a) and 8(b), a PC with a 1.5 ns time advance of the output envelop pulse maximum, compared to the considered input envelop.

It is important to note that the gain of the voltage plots shown in Figure 6 is lower than that of Figure 8 because the frequency spectrum of the input signal shown in Figure 8 is larger (inversely proportional to the time-domain pulse width). So, according to “V” form of the gain, it enables to interact with wider bandwidth where the gain is

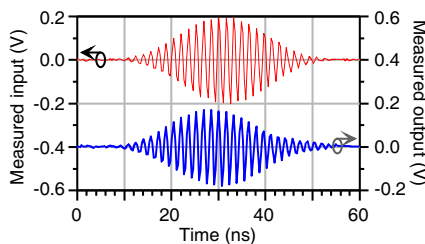


Figure 6. Time-domain experimental results of the circuit shown in Figure 4 for the modulated Gaussian input pulse with 8.4 ns standard deviation and a carrier frequency at 622 MHz.

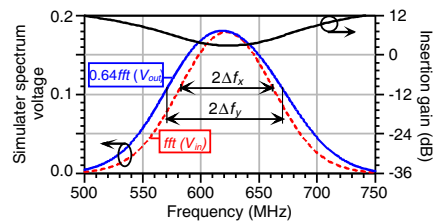


Figure 7. Simulated input- and output-voltage Fourier transforms yielded from the measured S -parameters.

higher.

To demonstrate the feasibility of this compression technique at higher frequencies, another prototype consisting of a two-stage of NGD circuit that operates at about 1 GHz was also investigated.

3.3. Evidence of Pulse Signal Compression with Two-stage NGD Device

Figure 9 represents the schematic of the fabricated two-stage NGD device [37, 38] fed at $V_{ds} = 3\text{ V}$ and $I_{ds} = 30\text{ mA}$. It is based on the use of the FET EC-2612 manufactured by Mimix BroadbandTM with the characteristics $g_m = 98.14\text{ mS}$ and $R_{ds} = 118.6\ \Omega$. To ensure input matching, a resistance $R_i = 75\ \Omega$, was connected in shunt at the input of the circuit.

The experimental results of the tested device presented in [37, 38] show an NGD in the frequency band around 300 MHz and centred at about 1.03 GHz. In addition, in this frequency band, the insertion gain displays the form favorable to exhibit pulse compression. As performed previously, the measured S -parameters were used to get a transient simulation with a modulated Gaussian input wave pulse

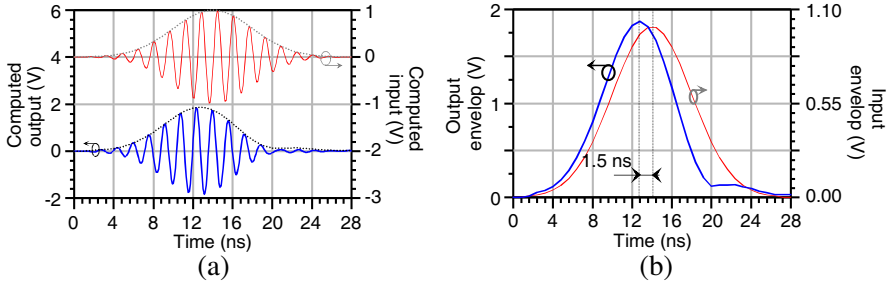


Figure 8. Results of simulations run with the measured S -parameters: (a) Transient- and (b) envelop-voltages.

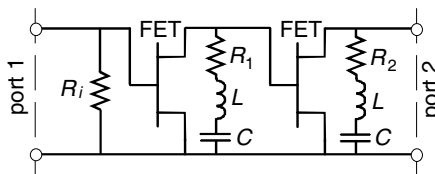


Figure 9. Schematic of the fabricated two-stage of NGD circuit using FET EC-2612, $R_m = 75\ \Omega$, $R_1 = 11\ \Omega$, $R_2 = 36\ \Omega$, $L = 12\text{ nH}$, $C = 1\text{ pH}$ [37, 38].

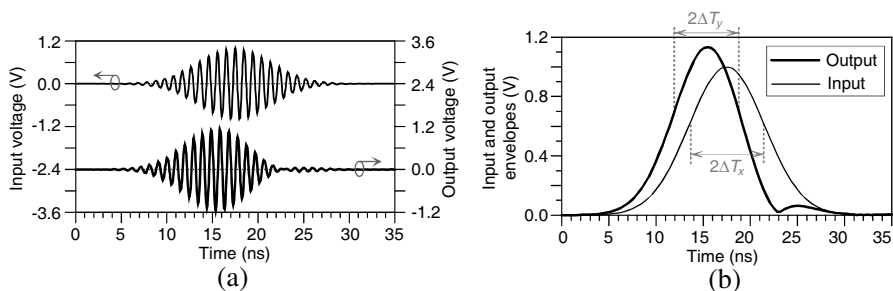


Figure 10. (a) Time responses simulated with the measured S -parameters and (b) the corresponding envelopes.

with $\Delta T_x = 4$ ns and centered at 1.03 GHz.

Figure 10(a) depicts the obtained results, and it shows that the output behaves also as a Gaussian wave pulse modulated at the same carrier frequency. Figure 10(b) demonstrates that, in addition to the advance of peak and fronts of the output envelopes, the pulse width compression, from $\Delta T_x = 4$ ns and $\Delta T_y = 3.5$ ns, is 87.5%.

4. CONCLUSION

A technique of microwave pulse signal compression for the modulated signal is reported. It is based on the use of an active cell composed of an FET in cascaded with shunt RLC resonant network. As introduced in [37–40], this cell generates a group delay always negative at its resonance frequency. In addition, as demonstrated in this paper that through analytical studies, because of its insertion gain form, this circuit is also susceptible to compress pulse RF signals.

Compared to the pulse compressors available in the literature [1–18], the technique reported here offers considerable benefits in terms of application. First, it is practically less complicated and can be implemented with compact-size devices; Furthermore, it presents a flexibility to operate both in narrow and as well as in wide frequency bands. The presented prototypes are with about $2\text{ cm} \times 2\text{ cm}$ dimensions and with cost lower than twenty euros in hybrid technology and hopefully cheaper in other technologies. Most importantly, compared to the topology of NGD active circuit used in [19], the topology presented in this paper is susceptible to operate at higher frequencies and integrable. This makes this technique potentially useful notably in microwave engineering as radar system applications.

To validate this concept, as proof-of-principle, two different prototypes of NGD hybrid planar circuit working at 622 MHz and

1.03 GHz were designed and tested. It was demonstrated that these devices generated an NGD and gain around their resonance frequencies. In addition, PC was successfully evidenced in time domain through the use of transient simulations executed with a commercial circuit simulator and based on measured S -parameters. When the prototypes were excited by a modulating Gaussian pulse with 4 ns standard deviation, it was proved that the widths of the output pulse are compressed about 80%.

Thanks to this compression function, the active circuit investigated is potentially interesting especially for the enhancement of the signal integrity through the reduction of the inter-symbol interference (ISI) in the numerical and telecommunication channels.

Investigation about the design of NGD pulse compressors and able to operate at higher frequencies through the use of distributed elements is in progress. I believe that, thanks to this compression function, it should be worth using the presented NGD topology to compensate for dispersion effects.

REFERENCES

1. Gaponov-Grekhov, A. V. and V. L. Granatstein, *Applications of High-power Microwaves*, Artech House, Boston, MA, 1994.
2. Thumm, M. K. and W. Kasparek, "Passive high-power microwave components," *IEEE Trans. Plasma Sci.*, Vol. 30, No. 3, 755–786, 2002.
3. Bromley, R. A. and B. E. Callan, "Use of a waveguide dispersive line in an f.m. pulse-compression system," *Proc. of IEE*, Vol. 114, 1213–1218, 1967.
4. Giordmaine, J. A., M. A. Duguay, and J. W. Hansen, "Compression of optical pulses (Mode locked HeNe laser generated light pulse compression in time without energy loss, using method similar to chirp radar method)," *IEEE J. Quantum Electron.*, Vol. 4, 252, 1968.
5. Strickland, D. and G. Mourou, "Compression of amplified chirped optical pulses," *Opt. Commun.*, Vol. 55, 447–449, 1985.
6. Li, P., X. Chen, Y. Chen, and Y. Xia, "Pulse compression during second-harmonic generation in engineered aperiodic quasi-phase-matching gratings," *Optics Express*, Vol. 13, No. 18, 6807–6814, 2005.
7. Arbore, M. A., O. Marco, and M. M. Fejer, "Pulse compression during second-harmonic generation in aperiodic quasi-phase-matching gratings," *Opt. Lett.*, Vol. 22, No. 12, 865–867, 1997.

8. Arbore, M. A., "Engineerable compression of ultrashort pulses by use of second-harmonic generation in chirped-period-poled lithium niobate," *Opt. Lett.*, Vol. 22, No. 17, 1341–1343, 1997.
9. Imeshev, G., "Engineerable femtosecond pulse shaping by second-harmonic generation with Fourier synthetic quasi-phase-matching gratings," *Opt. Lett.*, Vol. 23, No. 11, 864–866, 1998.
10. Wang, C. and J. Yao, "Photonic generation of chirped millimeter-wave pulses based on nonlinear frequency-to-time mapping in a nonlinearly chirped fiber Bragg grating," *IEEE Tran. MTT*, Vol. 56, No. 2, 542–553, 2008.
11. Wang, C. and J. Yao, "Photonic generation of chirped microwave pulses using superimposed chirped fiber Bragg gratings," *IEEE Photon. Technol. Lett.*, Vol. 20, No. 11, 882–884, 2008.
12. Zeitouny, A., S. Stepanov, O. Levinson, and M. Horowitz, "Optical generation of linearly chirped microwave pulses using fiber Bragg gratings," *IEEE Photon. Technol. Lett.*, Vol. 17, No. 3, 660–662, 2005.
13. Baum, C. E., "Coupling ports in waveguide cavities for multiplying fields in pulse-compression schemes," *Circuit and Electromagnetic System Design Note*, 52, 2006.
14. Augustinovitch, V. A., S. N. Artemenko, P. Y. Chumerin, V. L. Kaminsky, V. L. Novikov, Y. G. Yushkov, and D. V. Zeltsov, "Circuit designs in microwave pulse compression," *Proc. of International Vacuum Electronics Conference Abstracts*, 2, 2000.
15. Burt, G., S. V. Samsonov, A. D. R. Phelps, V. L. Bratman, K. Ronald, G. G. Denisov, W. He, A. R. Young, A. W. Cross, and I. V. Konoplev, "Microwave pulse compression using a helically corrugated waveguide," *IEEE Trans. on Plasma Science*, Vol. 33, No. 2, 661–667, 2005.
16. Danilov, Y. Y., S. V. Kuzikov, V. G. Pavel'ev, Y. I. Koshurinov, and D. Y. Shchegol'kov, "Linear frequency-modulated pulse compressor based on a three-mirror ring cavity," *Tech. Phys. Lett.*, Vol. 50, No. 4, 523–525, 2005.
17. Petelin, M., J. Hirshfield, Y. Y. Danilov, S. Kuzikov, V. Pavelyev, D. Schegolkov, and A. Yunakovsky, "Components for quasi-optically-fed linear accelerators," *Proc. of AIP Conf.*, Vol. 807, 408–415, 2006.
18. Kuzikov, S. V., Y. Y. Danilov, G. G. Denisov, D. Y. Shegokov, and A. A. Vikharev, "Multi-mode sled-II pulse compressors," *Proc. of LINAC2004*, THP28, 660–662, Lübeck Germany, 2004.

19. Cao, H., A. Dogariu, and L. J. Wang, "Negative group delay and pulse compression in superluminal pulse propagation," *IEEE J. Sel. Top. Quantum Electron.*, Vol. 9, No. 1, 52–58, 2003.
20. Lucyszyn, S., I. D. Robertson, and A. H. Aghvami, "Negative group delay synthesiser," *Electronic Lett.*, Vol. 29, 798–800, 1993.
21. Broomfield, C. D. and J. K. A. Everard, "Broadband negative group delay networks for compensation of oscillators, filters and communication systems," *Electronics Lett.*, Vol. 23, 1931–1933, 2000.
22. Eleftheriades, G. V., O. Siddiqui, and A. K. Iyer, "Transmission line for negative refractive index media and associated implementations without excess resonators," *IEEE MWC Lett.*, Vol. 13, No. 2, 51–53, 2003.
23. Siddiqui, O. F., M. Mojahedi, and G. V. Eleftheriades, "Periodically loaded transmission line with effective negative refractive index and negative group velocity," *IEEE Trans. Ant. Prop.*, Vol. 51, No. 10, 2619–2625, 2003.
24. Siddiqui, O. F., S. J. Erickson, G. V. Eleftheriades, and M. Mojahedi, "Time-domain measurement of negative group delay in negative-refractive-index transmission-line metamaterials," *IEEE Trans. MTT*, Vol. 52, 1449–1454, 2004.
25. Chiao, R. Y., E. L. Bolda, J. Bowie, J. Boyce, and M. W. Mitchell, "Superluminality and amplifiers," *Prog. Crystal Growth Charact. Mat.*, Vol. 33, 319–325, 1996.
26. Mitchell, M. W. and R. Y. Chiao, "Causality and negative group delays in a simple bandpass amplifier," *Am. J. Phys.*, Vol. 66, 14–19, 1998.
27. Mitchell, M. W. and R. Y. Chiao, "Negative group delay and 'fronts' in a causal systems: An experiment with very low frequency bandpass amplifiers," *Phys. Lett. A*, Vol. 230, 133–138, 1997.
28. Kitano, M., T. Nakanishi, and K. Sugiyama, "Negative group delay and superluminal propagation: An electronic circuit approach," *IEEE J. Sel. Top. Quantum Electron.*, Vol. 9, No. 1, 43–51, 2003.
29. Nakanishi, T., K. Sugiyama, and M. Kitano, "Demonstration of negative group delays in a simple electronic circuit," *Am. J. Phys.*, Vol. 70, No. 11, 1117–1121, 2002.
30. Solli, D., R. Y. Chiao, and J. M. Hickmann, "Superluminal effects and negative group delays in electronics, and their applications," *Phys. Rev. E*, Vol. 66, 056601.1–056601.4, 2002.

31. Munday, J. N. and R. H. Henderson, "Superluminal time advance of a complex audio signal," *Appl. Phys. Lett.*, Vol. 85, 503–504, 2004.
32. Woodley, J. F. and M. Mojahedi, "Negative group velocity and group delay in left-handed media," *Phys. Rev. E*, Vol. 70, 046603.1–046603.6, 2004.
33. Pendry, J. B., "Negative refraction make a perfect lens," *Phys. Rev. Lett.*, Vol. 85, 3966–3969, 2000.
34. Shelby, R. A., D. R. Smith, and S. Schultz, "Experimental verification of a negative index of refraction," *Science*, Vol. 292, 77–79, 2001.
35. Pendry, J. B., "Negative refraction," *Contemporary Physics*, Vol. 45, 191–202, 2004.
36. Smith, D. R., J. B. Pendry, and M. C. K. Wiltshire, "Metamaterials and negative refractive index," *Science*, Vol. 305, 788–792, 2004.
37. Ravelo, B., A. Perennec, M. Le Roy, and Y. Boucher, "Active microwave circuit with negative group delay," *IEEE MWC Lett.*, Vol. 17, No. 12, 861–863, Dec. 2007.
38. Ravelo, B., A. Perennec, and M. Le Roy, "Synthesis of broadband negative group delay active circuits," *IEEE MTT-S Int. Symp. Digest*, 2177–2180, Jun. 2007.
39. Ravelo, B., A. Perennec, and M. Le Roy, "Negative group delay active topologies respectively dedicated to microwave frequencies and baseband signals," *J. EuMA*, Vol. 4, 124–130, Jun. 2008.
40. Ravelo, B., A. Perennec, and M. Le Roy, "Study and application of microwave active circuits with negative group delay," *Microwave and Millimeter Wave Technologies Modern UWB Antennas and Equipment*, Chapter 21, Intech Book ed. by Prof Igor Minin, 415–439, Mar. 2010.